Available online at www.sciencedirect.com
SCIENCE DIRECT
Surface Science 600 (2006) 1849–1853
SURFACE SCIENCE
www.elsevier.com/locate/susc

Alumina supported model Pd–Ag catalysts: A combined STM, XPS, TPD and IRAS study

N.A. Khan *, A. Uhl, S. Shaikhutdinov, H.-J. Freund

Department of Chemical Physics, Fritz-Haber-Institut der Max-Planck-Gesellschaft, Faradayweg 4-6, 14195 Berlin, Germany

Received 2 December 2005; accepted for publication 10 February 2006
Available online 3 March 2006

Abstract

The bimetallic Pd–Ag model catalysts were prepared by physical vapor deposition on thin alumina films. The morphology and structure of the Pd–Ag particles were studied by STM, XPS, and by TPD and IRAS of CO. The results showed the formation of true alloy particles with Ag segregated at the surface. The addition of Ag first suppresses the most strongly bonded CO on threefold hollow sites of Pd. With further increasing Ag coverage, only isolated Pd atoms surrounded by Ag atoms are likely present on the surface. The results on CO adsorption suggest that the model Pd–Ag system mimics the structure of the real Pd–Ag catalysts.

Keywords: XPS; STM; IRAS; Bimetallic; Palladium; Silver; CO

1. Introduction

Pd-based catalysts are commonly used as hydrogenation catalysts in industry. In many cases, the Pd-based alloy catalysts exhibit higher selectivity than the pure Pd catalysts [1–5]. Specifically, the Pd–Ag systems have generated an immense amount of interest for use in hydrogen membranes [6] and as selective hydrogenation catalysts [2,7]. Particularly, Pd–Ag catalysts are used in the selective hydrogenation of acetylene in the excess of ethylene in feedstock for ethylene polymerization [8]. However, the role of Ag in these catalysts is difficult to investigate experimentally because of low metal loading, typically ~1 wt.% [3,8,9].

The physical and electronic properties of the bulk Pd–Ag alloy systems have been studied both experimentally and theoretically [10–13]. Surface science studies of Pd–Ag single crystals indicate that surface segregation of Ag reduces the surface composition of Pd to less than 10% [10,11]. However, the extent to which Ag segregates depends on the temperature, preparation conditions, the external environment (oxidizing or reducing) and the internal environment (bulk alloy vs. thin film) [14]. Theoretical studies of Pd–Ag clusters also showed that depending on the structure of the cluster and the temperatures at which they are grown, the segregation properties of the Ag–Pd particles can vary [15,16]. Surface segregation can strongly influence the adsorption properties of bimetallic compounds and hence their reactivity [17,18].

In order to understand the origin of beneficial effects of Ag on the Pd hydrogenation catalysts, we study planar model systems, where the highly sensitive surface science techniques allow one to characterize the structural, electronic and adsorption properties of the Pd–Ag particles under controlled conditions. In this paper, we employ scanning tunneling microscopy (STM), X-ray photoelectron spectroscopy (XPS), temperature programmed desorption (TPD) and infrared reflection absorption spectroscopy (IRAS) of CO as a probe molecule for structural characterization of the Pd–Ag nanoparticles deposited on thin alumina films.

* Corresponding author. Present address: National Energy Technology Laboratory (NETL), 626 Cochrans Mill Rd., Pittsburgh, PA 15236, USA.
E-mail address: Neetha.Khan@netl.doe.gov (N.A. Khan).

0039-6028/$ - see front matter © 2006 Elsevier B.V. All rights reserved.
doi:10.1016/j.susc.2006.02.016

2. Experimental

The experiments were performed in three different UHV chambers (the base pressure below 5×10^{-10} mbar). All chambers were equipped with low-energy electron diffraction (LEED), a differentially pumped quadrupole mass spectrometer (QMS), and facilities for sample cleaning and preparation. All gases were introduced to the crystal using a calibrated directional gas doser.

The alumina film was grown on a clean NiAl(1 1 0) single crystal by two cycles of oxidation at 10^{-6} mbar of O_2 at 550 K for 20 min and annealing to 1140 K for 5 min. The quality of the alumina film was confirmed by observation of a characteristic LEED pattern with sharp diffraction spots [19].

Palladium and silver were deposited on the alumina film using an electron-beam assisted evaporator (Focus EFM3). The coverage of Pd and Ag is reported as a nominal thickness (in Å). The deposition rate was ~0.2 Å/min for both metals, as calibrated in situ using a quartz microbalance. In these experiments, the metals were deposited while the substrate was kept at ~90 K. After deposition, the sample was flashed to ~380 K to desorb any background hydrogen that may adsorb during deposition. In order to further stabilize the particles before CO TPD and IRAS measurements, the sample was then oxidized for ~10 min in 10^{-6} mbar O_2 at 500 K. This procedure has been shown to grow a thicker oxide film that prevents Pd from diffusing into the oxide film at elevated temperatures [20]. The particles were reduced by CO until no CO_2 can be detected in CO TPD spectra. IRAS and TPD measurements taken on pristine Pd and Pd–Ag particles and the particles after the oxidation/reduction procedure do not exhibit any new features, indicating the surfaces are similar. These treatments are assumed to simulate the calcinations/reduction procedures while preparation of the real catalysts.

3. Results and discussion

Fig. 1 shows STM images of Pd (a), Ag (b) and Pd–Ag (c) particles formed by vapor deposition of metals onto the alumina film. It is clearly seen that Ag forms larger particles than Pd due to a weaker interaction of the Ag adatoms with the alumina film. The different nucleation and growth mode of metals can help to distinguish the nature of the particles imaged by STM when metals are co-deposited as has been previously shown in our group for the Pd–Co system [21,22]. For co-deposited Pd–Ag systems, the morphology is very similar to the pure Pd system indicating that nucleation and growth of Pd–Ag particles is governed by the interaction of Pd with this support whereby the Ag atoms stick to the nucleating Pd particles, thus forming bimetallic particles rather than individual Ag particles between the Pd particles.

XPS inspection of the Pd–Ag samples has revealed a significant negative binding energy shift (−0.7 eV) of the Ag 3d core level in the Pd–Ag samples as compared to pure Ag particles, as shown in Fig. 2. Such effects were previously reported on bulk and surface Pd–Ag alloys, both experimentally and theoretically [23–25]. The results suggest that charge transfer may have occurred and the complete screening picture may be applicable. Theoretical calculations also indicate that both Pd and Ag gain *d* and lose non-*d* charge when alloyed with each other [26]. For the present study, our XPS results show similarities with the bulk alloy systems, indicating that the formation of true alloy Pd–Ag particles on the alumina film has occurred.

The CO adsorption on pure Pd particles has been studied previously in detail [27,28]. Weakly-bound linear (or atop) CO species desorb first, resulting in a broad TPD signal at 100–300 K [20]. As the CO coverage decreases on heating, the remaining molecules occupy the more favorable bridge and threefold hollow sites from which they desorb at a higher temperature (HT) with a well-resolved maximum at ~470 K as shown in Fig. 3.

When the smallest amount (0.1 Å) of Ag is co-deposited with Pd, the HT peak decreases in intensity and a new peak at low temperature (LT), ~120 K, appears. The LT peak gains intensity but then starts to decrease after 0.4 Å Ag has been deposited, meanwhile the HT peak continually decreases. These results are consistent with TPD studies of Nieuwenhuys and co-workers [10,12] on a PdAg(1 1 1) single crystal. In this work, the authors showed that an alloy surface with bulk concentration of 67%Pd–33%Ag in fact exhibited surface composition of 10%Pd–90%Ag and a single CO desorption peak at

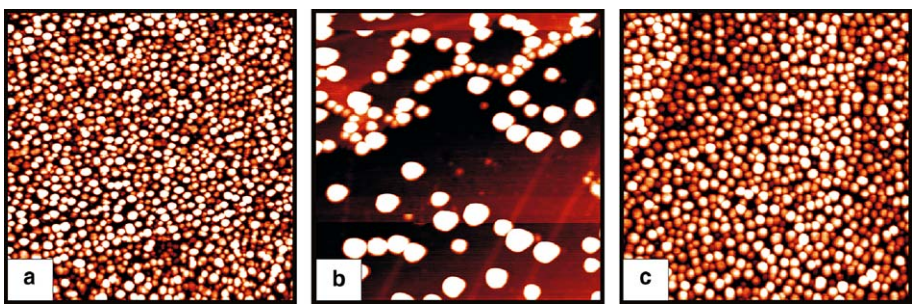

Fig. 1. Room temperature STM images of 2 Å Pd (a), 2 Å Ag (b) and 2 Å Pd + 0.4 Å Ag (c) deposited on alumina film at 100 K (image size 100×100 nm^2).

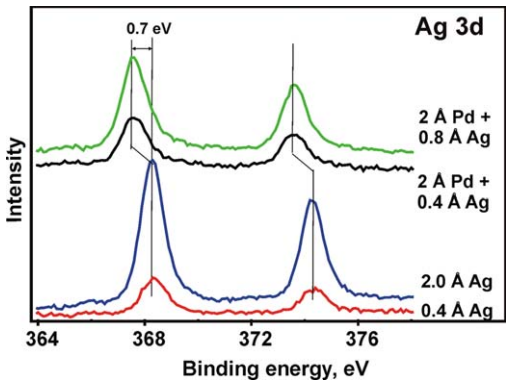

Fig. 2. Ag 3 d region of XPS spectra for alumina supported Ag and Ag–Pd particles.

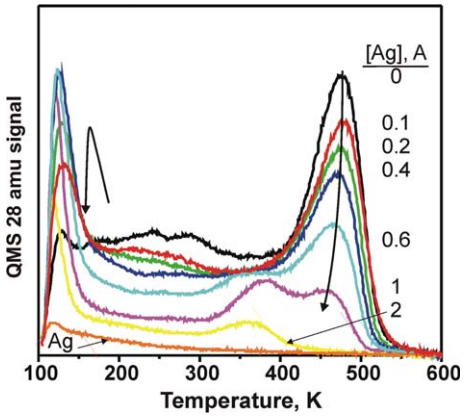

Fig. 3. TPD spectra of 2 L of CO exposed to Pd–Ag/alumina particles at 100 K as a function of Ag co-deposited with 2 Å of Pd as indicated.

375 K. The presence of Ag on the surface suppresses the HT desorption peak, attributed to the threefold hollow sites on Pd(1 1 1). The high surface concentration of Ag leads the authors to propose that only isolated Pd atoms, surrounded by Ag atoms, are present on the surface. This finding has been corroborated by Wouda et al. [11] using STM with atomic resolution. If we compare this single crystal surface to the Pd–Ag particles with the bulk ratio 2:1 used in our experiments, we also observe a similar situation, where the HT desorption peak vanishes and a peak at ~375 K emerges.

It is well known that the stretching frequency of CO depends on the nature of adsorption site on the metal surface. CO adsorbed at threefold hollow sites of Pd results in the IR signals between 1820 and 1920 cm^{-1} with a continuous shift toward higher frequencies as the CO coverage increases. Accordingly, a signal centered at ~1960 cm^{-1} is assigned to bridge-bonded CO, which emerges at intermediate coverage. Finally, at saturation coverage reached at low temperatures (around 100 K), atop species are populated giving rise to a signal at around 2105 cm^{-1} [27,29].

Fig. 4 shows IRAS spectra of the Pd–Ag particles at saturation CO coverage as a function of amounts of Ag co-deposited with 2 Å of Pd. Adding even the smallest

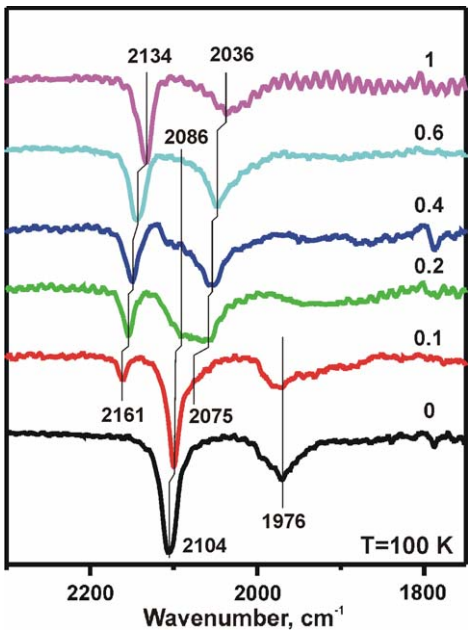

Fig. 4. IR spectra of 2 L of CO adsorbed on Pd–Ag particles at 100 K as a function of amounts of Ag added to 2 Å Pd as indicated.

amounts of Ag (Ag:Pd ratio is 1:20) show new features in the spectra as compared to pure Pd. At 100 K, a peak at ~2161 cm^{-1} is clearly seen which gains intensity with increasing Ag coverage up to 1 Å. The peak at 2104 cm^{-1} assigned to atop CO species on Pd shifts to lower frequencies and gradually attenuates at higher Ag coverage. In addition, a new absorption band develops from a low-frequency shoulder at ~2075 cm^{-1} of the atop Pd species to the well-resolved peak at higher Ag coverage. Finally, the band assigned to bridge-bonded CO on Pd (2000–1950 cm^{-1}) has been strongly attenuated as compared to pure Pd particles.

In order to further correlate the IR and TPD results we have recorded IRAS spectra after the sample was flashed to the specified temperature. Fig. 5 shows data for the pure Pd (a) and Pd–Ag particles with low (b) and high (c) Ag concentrations. It is clear that Ag-induced CO species, exhibiting frequencies of 2154 and 2134 cm^{-1}, desorbs first, that correlates with CO TPD peak at ~120 K. Then CO species at 2086 cm^{-1} (observed only at low Ag coverage) disappears upon heating to 300 K, which corresponds to a broad TPD signal at 150–300 K. Meanwhile, the peaks at 2058 and 2048 cm^{-1} stay unless the sample is heated to 400 K. This nicely correlates with the TPD peak at 375 K (see Fig. 3). The bands below 1950 cm^{-1}, which are present only at low Ag coverage, behave very similar to those on pure Pd particles and therefore can be straightforwardly assigned to CO adsorbed on bridge and threefold hollow sites of Pd, respectively.

Therefore, the data clearly show that two CO adsorption species, which are characterized by $\nu = 2105$–2085 cm^{-1} ($T_{des} = 100$–300 K), and $\nu = 1900$–1800 cm^{-1} ($T_{des} = 400$–500 K) are essentially identical to those observed on the

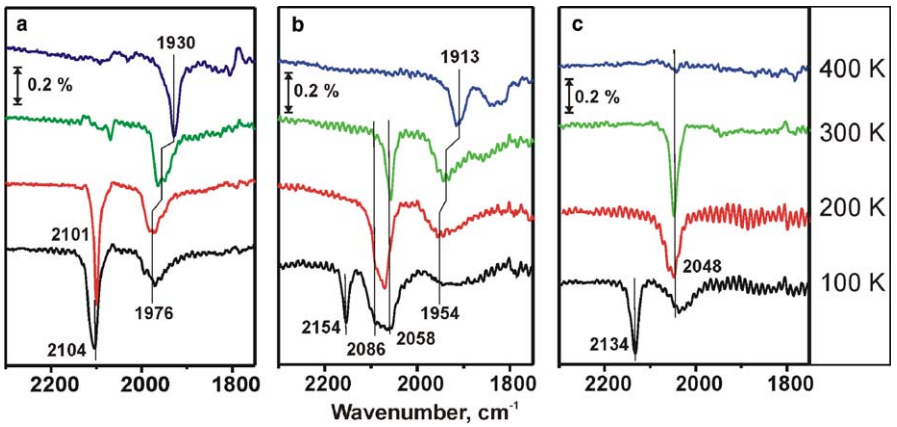

Fig. 5. IR spectra of CO adsorbed at 100 K on pure 2 Å Pd (a), co-deposited 2 Å Pd + 0.2 Å (b) and 1 Å (c) of Ag, then annealed to the indicated temperature.

pure Pd particles and therefore can be assigned to CO adsorbing on islands or domains of Pd present on the surface of the Pd–Ag particles, the abundance of which is reduced with increasing Ag concentration.

Adding Ag results in two new CO species: weakly-bound ($T_{des} \sim 120$ K) with $\nu \sim 2160$–$2135\ cm^{-1}$, and more strongly bound ($T_{des} \sim 375$ K) with $\nu \sim 2075$–$2035\ cm^{-1}$. The high frequency band, which is blue-shifted with respect to CO in gas phase, was previously observed on Ag films for CO adsorbed only below 50 K and therefore assigned to physisorbed CO [30]. However, Rodriguez et al. observed similar IR features for Ag sub-monolayer films on a Pt(1 1 1) substrate when exposed to CO at 90 K [30,31]. Since in our experiments we have not observed any CO adsorption on pure Ag particles at 90 K, both Rodriguez's and our findings indicate that CO adsorbs more strongly on the Ag atoms in the presence of Pd (Pt) surrounding. (It should be mentioned that the IR signal at $\sim 2150\ cm^{-1}$ has been observed on silica supported Ag catalysts under realistic conditions [32]. The authors have assigned this band to CO–$Ag^{\delta+}$ species, where Ag may be partially oxidized following calcination treatment, which is definitely not the case in our experiments.)

The origin of another IR feature at 2075–$2035\ cm^{-1}$ (see Fig. 4) is not obvious. This CO species stays in a wide range of the Ag coverage and desorbs above 300 K (see Fig. 5). At a Pd–Ag ratio of 2:1, the TPD spectra clearly show a peak at ~375 K (see Fig. 3), which has been also observed on the Pd–Ag single crystals [10]. Note that CO at bridge and threefold hollow sites on pure Pd is not present in any spectrum with this Ag coverage (see Fig. 5c), indicating that there are little or no adsorption sites with more than one Pd atom present. In addition, the position of this peak is rather independent of the temperature (and hence of CO coverage), which implies isolated CO species, which in turn can explain their desorption in a single peak at 375 K as observed by TPD (see Fig. 3).

For Pd–Au and Pd–Cu particles supported on 2–3 nm thick alumina films grown on Mo(1 0 0), Rainer et al. observed an IR band at ~2085 (for Au) cm^{-1} and $\sim 2060\ cm^{-1}$ (for Cu) which they attributed to CO linearly-bonded to a "diluted" Pd on the surface [33]. The authors argue that this feature can hardly be associated with CO multiply bonded to Pd and Au (Cu) as the stretching frequency is too high. In addition, they found that this peak behaves similarly to atop CO bound on Pd in an uncompressed CO overlayer. Therefore, we may also suggest that the band at $\sim 2060\ cm^{-1}$ for Pd–Ag particles is likely due to CO linearly adsorbed on isolated Pd atoms surrounded by Ag atoms. On the other hand, the desorption temperature of these species (~375 K) is even higher than for CO adsorbed on top of Pd in pure Pd particles, which has desorbed by 300 K (see Fig. 5a). Therefore, we cannot rule out the possibility that this band is associated with CO bridge bonded between Pd and Ag surface atoms. However, theoretical calculations are necessary to clarify this issue.

Fig. 4 shows that that the IR signals are red-shifted at increasing Ag concentration. This may be due to decreasing CO coverage, as suggested by CO TPD results (see Fig. 3), which reduces CO–CO interaction. However, as discussed by Primet et al. [34] for room temperature CO adsorption on silica supported Pd–Ag catalysts of various composition, this shift must be more attributed to a Ag-induced increase of electron density on the Pd surface atoms, which results in an increased Pd → CO back-donation.

In summary, the results shown here are consistent with the formation of alloy Pd–Ag particles, with Ag-rich surfaces. The core level shift in the XPS spectra supports the formation of alloy particles, but in addition, the CO TPD results provide further evidence that the particles are alloyed, and not core–shell particles. At Ag coverages below 2 Å, the presence of Pd in the surface of the particles is confirmed with the presence of the high temperature CO TPD peak. The IRAS also exhibits features consistent with Pd ensembles on the particles until Ag coverage is 1 Å or higher. Therefore, we conclude that we have Pd–Ag particles that are alloys with a preferential segregation of Ag to the surface. This is consistent with the segregation properties observed on the Pd–Ag single crystals [11]. This realization

is considerably important for Pd–Ag catalysts, as only 30% bulk Ag concentration in the Pd–Ag particles results in the formation of only single Pd adsorption sites. The effect of Ag on Pd is the blocking of CO adsorption on multiply coordinated sites, and the increase in linearly-bonded CO on the particles. Again, this is consistent with CO adsorption studies on supported Pd–Ag catalysts under more realistic conditions [9,34,35]. When performed at 300 K, these studies showed that Ag addition to the Pd catalyst increased the amount of more weakly-bound CO species. Essentially, the presence of Ag increases the ratio of linearly-bonded CO to the CO bonded to the bridge or threefold hollow site. This is exactly what is observed in Fig. 5 where the IR spectra of CO after flash to 300 K on Pd and Pd–Ag particles are compared. This comparison clearly shows that as the Ag content is increased, the population of linearly-bonded CO is strongly increased while the multi-coordinated sites of Pd are blocked. This close similarity between our model particles and real catalysts indicates that these particles can be used to ''mimic'' real catalysts.

4. Summary

The bimetallic Pd–Ag model catalysts supported on thin alumina films were studied by STM, XPS, and by TPD and IRAS of CO as a probe molecule. The results showed the formation of Pd–Ag alloy particles with Ag segregated to the surface. Adding Ag first suppresses the most strongly bonded CO on threefold hollow sites of Pd. With further increasing Ag coverage, only isolated Pd atoms surrounded by Ag atoms are likely to be present on the surface. The results on CO adsorption suggest that the model Pd–Ag system mimics the structure of the real Pd–Ag catalysts.

Acknowledgements

We acknowledge support by the Athena project funded by the Engineering and Physical Sciences Research Council (EPSRC) of the UK and Johnson Matthey plc. We also acknowledge Fonds der Chemischen Industrie and Deutsche Forschungsgemeinschaft. We also thank M. Naschitzki for the technical support. N.A. Khan acknowledges the Alexander von Humboldt Foundation for a fellowship.

References

[1] Q.W. Zhang, J. Li, X.X. Liu, Q.M. Zhu, Appl. Catal. A 197 (2000) 221.
[2] H. Zea, K. Lester, A.K. Datye, E. Rightor, R. Gulotty, W. Waterman, M. Smith, Appl. Catal. A 282 (2005) 237.
[3] D.C. Huang, K.H. Chang, W.F. Pong, P.K. Tseng, K.J. Hung, W.F. Huang, Catal. Lett. 53 (1998) 155.
[4] J.H. Kang, E.W. Shin, W.J. Kim, J.D. Park, S.H. Moon, J. Catal. 208 (2002) 310.
[5] L. Constant, P. Ruiz, M. Abel, Y. Robach, L. Porte, J.C. Bertolini, Top. Catal. 14 (2001) 125.
[6] J. Shu, B.E.W. Bongondo, B.P.A. Grandjean, A. Adnot, S. Kaliaguine, Surf. Sci. 291 (1993) 129.
[7] P.A. Sheth, M. Neurock, C.M. Smith, J. Phys. Chem. B 109 (2005) 12449.
[8] M.M. Johnson, D.W. Walker, G.P. Nowack, Phillips Petroleum Company, US Patent, 4,404,124, 1983.
[9] Y. Jin, A.K. Datye, E. Rightor, R. Gulotty, W. Waterman, M. Smith, M. Holbrook, J. Maj, J. Blackson, J. Catal. 203 (2001) 292.
[10] A. Noordermeer, G.A. Kok, B.E. Nieuwenhuys, Surf. Sci. 165 (1986) 375.
[11] P.T. Wouda, M. Schmid, B.E. Nieuwenhuys, P. Varga, Surf. Sci. 417 (1998) 292.
[12] G.A. Kok, A. Noordermeer, B.E. Nieuwenhuys, Surf. Sci. 152 (1985) 505.
[13] S. Jaatinen, P. Salo, M. Alatalo, V. Kulmala, K. Kokko, Surf. Sci. 529 (2003) 403.
[14] M. Ropo, K. Kokko, L. Vitos, J. Kollar, Phys. Rev. B 71 (2005) 045411.
[15] F. Baletto, C. Mottet, R. Ferrando, Phys. Rev. B 66 (2002).
[16] F. Baletto, C. Mottet, R. Ferrando, Phys. Rev. Lett. 90 (2003).
[17] J.R. Kitchin, N.A. Khan, M.A. Barteau, J.G. Chen, B. Yakshinksiy, T.E. Madey, Surf. Sci. 544 (2003) 295.
[18] B.C. Khanra, J.C. Bertolini, J.L. Rousset, J. Mol. Catal. A 129 (1998) 233.
[19] M. Bäumer, H.-J. Freund, Prog. Surf. Sci. 61 (1999) 127.
[20] S. Shaikhutdinov et al., Surf. Sci. 501 (2002) 270.
[21] M. Heemeier, A.F. Carlsson, M. Naschitzki, M. Schmal, M. Baumer, H.J. Freund, Ang. Chem. Int. Ed. 41 (2002) 4073.
[22] A.F. Carlsson, M. Naschitzki, M. Baumer, H.J. Freund, J. Phys. Chem. B 107 (2003) 778.
[23] P. Pervan, M. Milun, Surf. Sci. 264 (1992) 135.
[24] I.A. Abrikosov, W. Olovsson, B. Johansson, Phys. Rev. Lett. 8717 (2001) 176403.
[25] W. Olovsson, L. Bech, T.H. Andersen, Z. Li, S.V. Hoffmann, B. Johansson, I.A. Abrikosov, J. Onsgaard, Phys. Rev. B 72 (2005) 075444.
[26] I. Coulthard, T.K. Sham, Phys. Rev. Lett. 77 (1996) 4824.
[27] K. Wolter, O. Seiferth, J. Libuda, H. Kuhlenbeck, M. Bäumer, H.-J. Freund, Surf. Sci. 402–404 (1998) 428.
[28] T. Dellwig, G. Rupprechter, H. Unterhalt, H.J. Freund, Phys. Rev. Lett. 85 (2000) 776.
[29] K. Wolter, O. Seiferth, H. Kuhlenbeck, M. Baumer, H.-J. Freund, Surf. Sci. 399 (1998) 190.
[30] P. Dumas, R.G. Tobin, P.L. Richards, Surf. Sci. 171 (1986) 555.
[31] J.A. Rodriguez, C.M. Truong, D.W. Goodman, Surf. Sci. Lett. 271 (1992) L331.
[32] Z. Qu, S. Zhou, W. Wu, C. Li, X. Bao, Catal. Lett. 101 (2005) 21.
[33] D.R. Rainer, C. Xu, P.M. Holmblad, D.W. Goodman, J. Vac. Sci. Technol. A 15 (1997) 1653.
[34] M. Primet, M.V. Mathieu, W.M.H. Sachtler, J. Catal. 44 (1976) 324.
[35] A.E. Hamdaoui, G. Bergeret, J. Massardier, M. Primet, A. Renouprez, J. Catal. 148 (1994) 47.